

Nansen Symposium paper
Submitted to JGR OCEANS August, 1993

Ice-Ocean Interactions in the Greenland Sea Odden Region as
Interpreted in Ocean Mooring and Satellite Microwave Data

Frank D. Carsey
California Institute of Technology, Jet Propulsion Laboratory, Pasadena CA 91109

and

Andrew T. Roach
Applied Physics Laboratory, University of Washington, Seattle WA 98105

ABSTRACT

Satellite and in-situ data for the "Odden" region of the Greenland Sea are discussed with respect to describing regions of convection. The convection is discussed in terms of regional ice retreat, observed in passive microwave data, that has previously been associated with convection observed in ocean mooring data. These regions are tentatively identified in SAR data which shows plumes of about 300 m separation in an area about 20 km by 90 km immediately north of the rapidly retreating ice edge at the southern end of an ice edge embayment, taken to be the consequence of the flow of warm, saline Arctic intermediate Water to the surface during convection. Although there is no way to determine the depth of the convection it is assumed to be to intermediate depths. The embayment in 1989 is seen in passive microwave data to expand downwind at the rate expected of wind-forcing of either ice or surface water, but the actual mechanism at work is not known.

1. INTRODUCTION

1.1 Background

Ocean convection is seen as a globally important process in which air-sea interactions influence oceanic circulation through the production and ventilation of deep and intermediate waters. A key site of convection, active at least some winters, is in the Greenland gyre, and the convection seems to be related to the development of an ice feature called Odden ("the Icy Cape" in Norwegian), an eastward extension of the ice edge in the latitude range 71° to 75°N as shown in Figure 1 for the winter of 1989. Previously published results from the 1988-89 winter (Roach et al, 1993) showed that convection near the Odden ice edge at 75°N, 4°W immediately preceded the formation of the Nordbukta ("North Bay"), the central retreat ice cover embayment occurring nearly every winter.

The key dynamic elements of oceanic convection are taken to be the individual plumes, the clusters of plumes called chimneys, the eddies that are the consequence of chimneys aging in a rotating frame, and, in the Greenland Sea, the embayments and polynyas resulting from the outcropping and spread of uAIW convective return water on the surface. Recent numerical work, which has not included surface wind driving, has suggested that the chimneys, of scale 10-60 km, should grow through increase in plume numbers, decay through baroclinic instability, and circulate cyclonically with the gyre. Plumes are expected to have dimensions in the range of 100-1000 m; chimneys in the range 20-60 km; and eddies in the range 5-60 km (Jones and Marshall, 1993; Garwood, 1991; Gascard, 1991). In this paper we discuss these features as seen in satellite data. Specifically we present an interpretation of passive

microwave data for 1989 and 1992 in the context of a simple model of convection-driven ice-edge retreat causing Nordbukta growth with salinity constraints imposed by processes associated with the formation and migration of a small polynya. We also present SAR data which seems to describe the surface structure of convecting plumes and supports our hypothesis that convective action in an area at the ice edge controls the varying ice extent in this region.

1.2 The Odden Region

The oceanography of the Greenland-Iceland-Norwegian Seas has received much attention throughout the century, and here only a very quick overview is supplied; a comprehensive discussion of the region can be found in Hurdle (1986). The principal water masses involved in the Odden processes are the upper Arctic Intermediate Water (uAIW), a warmer saltier water of Atlantic origin, and the Polar Water (PW), a cooler fresher water of Arctic origin. The uAIW approaches the Greenland gyre from the northeast after moving north past Norway and curving west beneath Spitzbergen. Some of this flow is bathymetrically turned again to the east and forms the Greenland gyre with its center approximately at the location of GSP-4 in Figure 1. PW flows along the northwest side of the gyre moving in a southeasterly direction along Greenland as the Fast Greenland Current (EGC). Filaments of uAIW and PW forming the lower and upper branches of the Jan Mayen Current (JMC) flow to the south approximately along the ice edge before turning to the east, as shown in Fig. 1, to cut across the southern half of the gyre, and PW, freshened by seasonal sea ice melt, also forms the surface water of the Odden area (Bourke et al, 1992).

The uAIW is underlain, below about 500 m, with deeper waters that are cooler and slightly fresher than the uAIW, the Greenland Sea Deep Water (GSDW) and Norwegian Sea Deep Water (NSDW). These are the end-point waters for the Greenland Sea deep convection; their salinity ranges from 34.88 to 34.94 psu, and their temperatures from -0.5°C to -1.3°C , with the GSDW the fresher and cooler (see e.g. Johannessen, 1986).

1.3 Winter Processes in the Odden region

In winter the waters of the Greenland Sea are cooled by cold, mostly northerly and northeasterly winds. The waters at the surface of what will be Odden are buoyant with a mixed layer of uncertain depth, but perhaps some 75-100 m at end of summer, and this area will be cooled enough, in most winters, to form an ice cover. The uAIW water to the north has enough sensible heat that it does not form an ice cover. As Odden ice grows, brine is injected into the upper water increasing its salinity and density. This water will, if enough cooling and brine are supplied, convect into and sometimes through the uAIW water, and this process brings up convective return water with enough heat to stop ice formation or even melt ice, thus liberating fresh water (Killworth, 1979). If conditions are right convection will continue and deepen until it extends to the bottom, but this step is apparently not as simple as it sounds. In fact the deeply convecting water must have a salinity lower than the uAIW or it will not be compressible at depth (see Aagaard and Carmack, 1989). For deep convection, dynamical constraints must be met (Gascard, 1991). The issues of convection and deep water formation are examined in detail by Chu and Gascard (1991).

There is a temptation to think that the Odden ice growth simply converts the fresher surface PW to uAIW by brine generation, but this is not the case. The Bourke et al section shows a surface salinity change of about 1 psu/100 km; to remove this layer by brine from ice growth with the surface fluxes available is not practical. Specifically if we use a mean flux of 200 watts/m^2 and a mixed layer of 50 m mean thickness, the retreat of the edge of fresher layer, and thus of the ice edge, would

occur at a maximum (if all heat lost at the surface is latent heat, which it is not) of only 3 km/day, 20% of the observed rate (Roach et al, 1993, and below). Thus, the heat and brine in the convective-return uAIW is required. Considering that most of the surface heat loss goes into ocean cooling (Schott et al, 1993), the role of ice growth is limited to that of being the mixing engine bringing up the uAIW.

1.4 The Convective Events of 1989

As part of the Greenland Sea Project, oceanographic data from the upper 200 m at two locations were examined (Roach et al 1993; see also Schott et al, 1993). The growth of sea ice in the central Greenland gyre injected brine into the upper water column locally and reduced the vertical stability profile during December and January. Subsequent cooling increased the density of the surface waters to a critical point and a cold air outbreak in late January 1989 provided enough buoyancy loss to convectively overturn at least the upper 200m. Replacement water then rose from the warmer pool of intermediate water at mid-depth causing an increase in the heat available in the upper layer. The surface signature of that warming was the retreat of the ice cover near GSP-4 and then along the Greenland shelf edge to the southwest, where the warmer water apparently was advected. As will be discussed below the **meltback** estimated from sequential satellite images is about 11 km d^{-1} (or 13 cm s^{-1}), comparable to both the 10 cm s^{-1} mean current (measured by Foldvik et al. [1988] in the EGC at 79°N) and wind forcing of ice or surface water.

2 THE SATELLITE DATA

2.1 Data

To generate regional sea ice distribution we used image data from the Special Sensor Microwave Imager (SSM/I), an instrument designed to make a variety of oceanic and terrestrial observations (Hollinger et al, 1990), including the concentration and type of sea ice. SSM/I brightness temperatures (T_b) are acquired at 19, 37, 22 and 85.5 GHz at both polarizations except at 22 GHz. To obtain fine-scale data on ocean surface processes we used SAR data from the AMI on the ESA ERS-1 (Carsey, 1992); these radar images have resolution of about 30 m with swaths of 100 km.

2.2 SSM/I Interpretation

The interpretation of microwave radiance for new and young ice types is complex, and is different from the interpretation for thick first-year ice or older ice. The observed T_b for new and young ice depends on thickness according to whether the ice grows in calm or rough conditions. This situation has been examined using surface and satellite data (Grenfell et al, 1992) and with satellite data alone (Steffen and Maslanik, 1988). Essentially, nilas growth in calm water is characterized by a change from the low open sea T_b to the high ice T_b as a consequence of growth to only a few millimeters of thickness (Wensnehan et al, 1993), depending on frequency, while pancake ice growth in rough conditions is characterized by a nearly linear (albeit noisy) increase in T_b with ice thickness over the range 0 to about 15 cm, largely independent of frequency. Grenfell et al (1992) also noted that the vertically polarized radiance was enhanced for pancakes. Pancake ice has previously been indicated as the dominant form in the regions of the ice edge in the Odden region (see e.g., Tucker et al, 1991; Sutherland et al, 1989), and the meteorological conditions of this site are appropriate for this kind of growth (Weeks and Ackley, 1986). We assume that the Odden ice is principally pancake form. In a microscopic sense the microwave signal from pancake ice (as discussed in Grenfell et al 1992) may be the consequence of some variable, e.g., pancake wetness, that is

correlated to ice thickness rather than the consequence of ice thickness itself; on this there is no definitive data set or applicable model.

2.3 SSM/I Variables

To further examine the ice condition record we form the Polarization Ratio (PR) and the Gradient Ratio (GR), these variables have proven useful in the examination of the major ice types of the polar seas (Cavalieri et al, 1984).

$$PR(\lambda) = (T_{bV}(\lambda) - T_{bH}(\lambda)) / (T_{bV}(\lambda) + T_{bH}(\lambda))$$

$$GR = ((T_{bV}(37 \text{ GHz}) - T_{bV}(19 \text{ GHz})) / (T_{bV}(37 \text{ GHz}) + T_{bV}(19 \text{ GHz})))$$

where T_{bV} and T_{bH} are the vertically and horizontally polarized microwave brightness temperatures at the frequency indicated.

in the formation of PR and GR we have variables that have reduced sensitivity to surface temperature and weather, and we have also generated somewhat "tuned" variables as PR is more sensitive to open water fractional coverage or pancake thickness while GR is more sensitive to the presence of old ice although it is sensitive to open water as well (Cavalieri et al, 1984). From the definition of PR and GR their sensitivity to weather is reduced approximately by half, but it still can be appreciable. PR and GR are shown in Figure 2 for January 17, 1993 for a data set in which the 37 GHz data have been expressed on a 5 km grid which preserves the resolution at about 30 km. These data sets are consistent with the data for the entire winter, and they show that PR and GR are redundant variables of this ice cover, and we will use only PR to describe ice conditions,

2.4 The SSM/I Ice Edge

There are several interpretation schemes for Odden ice PR values. We could use the traditional approach in which thick ice is assumed and ice concentration is solved for (Steffen et al, 1992); we could utilize the Grenfell et al (1992) result and interpret PR as a pancake thickness for an area covered to some concentration by uniform-thickness pancakes; or we could acknowledge that there is a concentration ranging from 0-100% of variable thickness pancakes. While none of these is wholly satisfactory, the last category is doubtless more correct, but we do not have the information to pursue it quantitatively. The approach open to us is to assume, strictly for purposes of locating the ice edge, that the actual concentration and pancake thickness profiles along lines normal to the ice edge are essentially constant over the winter so that a suitable PR value is the locus of ice of essentially invariant spatial relationship to the ice edge,

3. THE 1989 and 1992 ODDEN EXTENT RECORDS

3.1 The 1989 Odden

The timing and strength of development of Odden is different in every year, and, in fact, it has not formed in some years (see Sutherland et al, 1989; Wadhams, 1986). The Odden in 1988-89 formed in November, reached maximum extent in December (Figure 1), and began to retreat in late January. The retreat took on its typical pattern as the formation of the Nordbukta at its northern edge near 75°N, 4°W. In the late winter-early spring time frame the Nordbukta can, as it did in 1989,

separate Odden from the EGC ice. Ice conditions in early spring were highly variable in 1989, and this is also typical.

3.2 Ice Retreat in 1989

In figure 3 the PR(37GHz) is shown for the Odden box of Figure 1 for the entire winter. According to Roach et al (1993) the convective events start about Jan 20, Shortly thereafter an **embayment** forms at the ice edge in the upper center of the Odden box, and the embayment grows by steady ice retreat of 10-15 km each day to the southwest (down in the box). the retreat continues steadily until about day 66 when there is some episodic alternation of PR increase and decrease. The tongue of ice that is the most persistent is seen to lie along the axis of the Jan Mayen Current (see Figure 1) as observed by Bourke et al (1992). In our analysis we assume that the Nordbukta retreat is the consequence of convection, to at least intermediate depth, beginning near the center of the Greenland gyre, occurring essentially annually.

Near day 30, three **small scallop-shaped embayments** appear in the ice edge, and these features migrate down the box, approximately to the southwest, We initially took them to be the chimney features as discussed by both theoretical (Jones and Marshall, 1993) and observational (Gascard, 1991) investigators, although the scale of the scallops is some 60-100 km (the uncertainty arising in uncertainty in SSM/I interpretation), larger than has been discussed. Another difficulty in the identification of the scallops as chimneys is that chimney drifts should retain the cyclonic sense of the gyre, but the scallops simply move to the southwest at the rate of the Nordbukta retreat.

The scallop which appears on the eastern side of the convective **embayment** does not simply move SW on the **embayment** fringe as the others do; it closes into a migrating open-water feature which we argue is basically a convective **sensible-heat polynya**, in figure 3 a yellow spot of 60-90 km diameter, When it has moved some 120 km to the SW of its formation another scallop forms at its origination site. The migrating **polynyas** "fill" with ice at approximate] y the northern edge of the JMC. It maybe that the upper PW filament of the JMC supplies enough fresh water to terminate the convection and permit formation of an ice cover once the heat pulse brought to the surface by the convection has been lost to the air. This feature has a distinct observable general behavior. Also, it is large enough that the SSM/I data should reasonably resolve its brightness, and the Tb data indicate a polarization intermediate between open water and a high concentration of thick pancakes; thus, this eastern polynya may be partially or completely filled with thin pancakes and may be difficult or impossible to observe in radar or visible-light data sets, or even visually from a ship's deck.

All the scallops move at within 10% of the rate of the Nordbukta retreat and are thus likely to be controlled by a common mechanism. At the same time, this tendency to move to the southwest is not universal to Odden-area features; the far northeast tip of Odden, for example, moves to the north-east; its behavior is **uncorrelated** with the **embayment** features.

3.3 The 1992 Odden

Figure 4 shows the 1992 Odden from SSM/I data, This was a winter in which the Odden formed late and was small, but there was the formation of Nordbukta a bit later than 1989. This data set is being used for comparison with ERS-1 SAR data, and in what follows SAR data for the rectangular area outlined in 4B will be discussed,

4. ODDEN ICE COVER BEHAVIOR

4.1 A Simple Model of Ice Retreat

We would like to develop a quantitative picture of the processes at work in the Greenland Sea convection. From the discussion of Roach et al, 1993, it seems that the rapid ice retreat is a signal feature of the convection and that this process must be the consequence of the sensible heat brought to the surface by the convective-return uAIW. The first question to address deals with the rate of ice retreat. From visual inspection of Figure 3 the ice retreat has a rate of about 12 km/day. The chimney growth rates suggested by theoretical analyses are 2-3 km/day (Legg and Marshall, 1993), and the currents of the region are negligible (Roach et al, 1993). Thus we have only the wind as external source for the rapid ice edge motion. If we speculate that the convective-return water terminates ice growth exactly, i.e., no ice at the ice edge is formed or melted after the convection begins, then the last ice that formed will move under simple wind forcing, and the open-water area will grow at that rate. To examine that prospect we use the Norwegian Hindcast winds for the location of GSP-4.

According to Moritz (1988),

$$U - c = BG \quad 1$$

where U is the (complex) ice velocity, c is the current, G is the geostrophic wind, and B is a complex constant which contains the drag coefficient and Coriolis turning. We will use $c = 0$. Further, we will concern ourselves only with the ice motion component down the center of the Odden box. Following Moritz (1988) we use

$$|B| = 1.21 \times 10^{-2} \quad 2$$

$$\Theta = \arg(B) = -3^\circ$$

In the above we are specifically modeling ice motion, but the modeling of the motion of warm surface uAIW would use equivalent terms (see McPhee, 1990). Thus, we are examining the motion of the ice edge to see if it is controlled by wind-driven properties, but we are not specifying what is being driven.

Figure 5 shows the geometry including a sample of geostrophic wind and ice motion down the box. Positive x-component of wind and ice motion are taken to be down the box. We generated daily average wind-forced and observed ice edge positions where the observed ice edge is the location, on the line down the box center, of PR=0. 12. Both resulting displacement series were smoothed for 7 days over the whole season. Figure 6 shows the resulting ice edge retreat velocity component by both SSM/I and the wind-forced calculation.

In interpreting Figure 6 errors must be considered, there are errors in the winds; there are geophysical variations in the parameters of 1 and 2; there may be local surface currents so that $c \neq 0$; and there are errors in Earth-location for the SSM/I data. For an uncorrelated uncertainty of 25 % for each, a fairly conservative estimate (Brown, 1990), there is an uncertainty of about 45 % in the comparison. Thus, the specifics of the curves cannot be interpreted closely. In Figure 6 the ice edge is seen to be going upwind to NE early in the winter, consistent with expected early-season thermodynamic ice advance, Beginning at about the time of convection onset the two indications of ice edge motion agree within the error estimates. During this period there is a tendency for negatively correlated departures in the two

curves; an increase in predicted wind-driven retreat occurs with a decrease in SSM/I retreat, and vice-versa, suggesting an additional loss of ice cover by wind-induced mixing.

This calculation fails to disprove that wind advection is a control of ice retreat in mid and later winter, but it is neither strong enough to confirm wind-forcing nor to specify whether the ice at the edge is moving a bit faster than or more slowly than the edge itself, or if the ice itself might be growing or becoming thinner near the edge. These considerations are important to the surface salinity budget. In the late winter the SSM/I ice edge becomes erratic as ice covers and retreats from large areas very quickly. In this situation the wind-forced model is too simple,

4.2 Refinements of Odden Behavior

Two events of the Odden arc advective, possibly wind-forced, and convective, the Nordbukta and the eastern polynya. It would be possible for the Nordbukta to be formed entirely by a convective-return water source limited in geographic extent to an area at the gyre center immediately around GSP-4; the convective-return water would simply be blown downwind to lose heat to the air while it mixes with local PW and uAIW. However, the eastern polynya has to bring its source of convective-return water with it as it moves to the southwest down the box. Thus we speculate that the convection in both the Nordbukta and the eastern polynya is confined to a region near the ice edge. Additionally, since ice is found all around the eastern polynya, in particular to the northeast, there must be, to stabilize the column, surface water with reduced salinity after the convection has moved on. This fresh water could be residual PW, or it could be the consequence of the melt of ice advected from the NE. The ice edge may moving more slowly than the ice, so that ice is always forming at the lower edge of the polynya, providing brine for convection, and melting at the upper edge. Thus, the data lead us to hypothesize that the convective water is located in, and confined to the southern end of, the open water area; the remainder of the Nordbukta and the eastern polynya are modified uAIW of convective-return origin.

Figure 3 permits a rough but useful calculation. From the rate of motion of the polynya, a given spot on the ocean is in the polynya for 8-10 days as the polynya is 100-120 km across and is moving at about 12 km/day. For mean fluxes of about 200 w/m², a 1 °C change in temperature would indicate a mixed layer of 40 m. The actual cooling is not known and may be smaller than 10 by as much as half, and the mixed layer is not well defined, but is in the range of 50-100 m (Bourke et al, 1992). Thus the heat loss by the ocean is consistent with the cooling of the mixed layer that has been warmed by mixing with uAIW as long as the uAIW-PW resultant water is fresh (stable) enough, which seems to be the case. At the point of origin of the eastern polynya the process of initiation of convection seems to be cyclical on approximately a 10 day period. At this site there is apparently refreshment of the surface water.

Although the Greenland Sea situation is explicitly not covered by the simulation, Killworth (1979) has examined convection in the Weddell Sea, and has suggested that convection in the presence of ice can take on a form in which the ice cover is intermittent. In this mode surface cooling causes the sea surface to freeze, and ice grows until the stability is destroyed, and then convection begins. The convection brings up warm water from depth; the warm water melts some or all the ice, and the convection is terminated until the melt-induced buoyancy is destroyed by ice growth whereupon the convection restarts. In Killworth (1979) this sequence is called ABCDA. For the Weddell Sea data the predicted ice cover is cyclic with a frequency about 1.2 day⁻¹. In Figure 7 we show a sample of individual passes of SSM/I over Odden; there are about 3 per day that cover the region reasonably well, and this rate spans frequencies adequately, considering that no intermittence is

visible in the daily data. The polynya is not seen to be changing in size or shape on the time scale of the satellite revisit schedule which suggests that the polynya is responding to mechanisms other than the intermittent-ice mode suggested by Killworth although the possibility of chimney-scale (5-10 km) intermittence on the polynya edge is not ruled out at the SSM/I resolution. The capability of the point of origin of the polynya to generate another polynya in about 10 days may be related to the Killworth processes in that the water at the ice edge has increasing salinity due to ice growth until convection is triggered,

5. CONVECTIVE PLUMES IN THE SAR DATA

The key element of oceanic convection, the active plume, has as yet not been convincingly observed or simulated. Some data has been acquired: from the temperature series on GSP 4 during the convective period, an upper bound on the vertical velocity of 3.1 cm s^{-1} was noted. This is in general agreement with vertical velocities measured directly by Doppler profilers in the Mediterranean Sea and in the Greenland Sea (Schott and Leaman, 1991; Schott et al, 1993). The modeling community has made great strides in determining what one can expect to find in the ocean. In particular, Jones and Marshall (1993) and Garwood (1991), through scaling arguments, have found the important terms in the convective process are buoyancy flux, Coriolis force and ocean depth. The Jones and Marshall (1993) calculations applied to our data with a nominal 500 W m^{-2} peak heat loss (for initiation of convection) yield a plume of about 160 m diameter with a vertical velocity of 2.2 cm s^{-1} while the Garwood approach finds that the plume array should have spacing dependent on convection depth and ranging up to 2 km for deep convection in the Greenland Sea, ERS-1 SAR data and modeling results are shown in Figure 8 (see also Carsey and Garwood, 1993); these figures are hypothesized to represent modeled and observed plume surfaces. The model result is from Garwood (1991) for deep convection; thus the SAR data indicate intermediate convection to 500-1000 m. The (hypothesized) convecting region is seen to be about 20 km by 90 km and to be located directly above the Odden ice edge. According to the ECMWF wind analysis for this area, the date of the SAR image, Feb. 12, 1993, was a day of very low winds, about 2 ms^{-1} ; in more usual wind conditions the plumes might have a very different appearance as well as structure,

Since the images of Figures 3 and 7 for 1989 indicate that the scallop-shaped embayments and the polynya are most likely all the same phenomenon at work, we can count embayments e.g., on day 38, to estimate that there are 3 or perhaps 4 regions of convection in Odden. In the images of Figure 4 for 1992 the scallop-shaped features are not as clearly shown, but one could argue that there are 2 such features present. In the 1989 data the points of origin of the embayments are apparently near the upper edge of Odden about $75^{\circ}\text{N}, 4^{\circ}\text{W}$. The site of origination of the eastern polynya is capable of sequential generation of the transient embayment convection. The retreat of the ice edge makes the SSM/I data useless as to sequences of convection away from the ice edge, e.g., at GSP4 after the ice has started to retreat, but the association this convection with the ice edge seems to argue against sequences in the other locations, An interesting issue with respect to comparison of the 1989 data with the model results of Legg and Marshall (1993) is whether the 3 embayments clearly visible in day 28 started off as one convective event which grew and subdivided into three as in their Figure 9; we suspect that they did but cannot be firm.

6. CONCLUSIONS

Modeled and observed convection behavior are integrated in Figure 9 which shows the processes of the central chimney and eastern polynya in cartoon form. The key features are the plumes, chimneys (aggregates of plumes), and open-water areas, the embayments and polynyas. The key difference between the eastern polynya and the Nordbukta is that the eastern polynya is advected as a closed chimney-like feature while the Nordbukta (the central retreat of Odden) is an embayment; a difference probably due to low surface salinity in the polynya area. We tentatively conclude that the Nordbukta has convection at work only in a few small regions (≤ 100 km) near the ice edge, and is characterized over most of the open-water area by a well mixed layer at least 200 m and possibly 500 m deep. We speculate that the eastern polynya is a convective, sensible-heat polynya that may be partly filled with ice; in-situ observations of this feature would be interesting and useful. The plumes observed in the Nordbukta seem to be small structures, about 100 m across, organized in an array with separation about 300 m, consistent with model results for intermediate convection. We would expect similar plumes to be active in the eastern polynya. We still have no model or strongly-indicative data on the mechanism for the propagation or wind-advection of convecting water although we hypothesize that the same mechanism is at work in both the Nordbukta and the eastern polynya. These tentative conclusions call for more data, from both satellite and in-situ platforms, and those data will advance the modeling work as well.

7. ACKNOWLEDGMENTS

SSM/I data are from NSIDC 'in boulder, and ERS-1 data are from ESA through ESRIN and the UK-PAF. We thank these archivists for their work and cooperative spirit. John Crawford and I-Lin Tang at JPL performed analysis tasks on the data sets. Knut Aagaard has been a source of good advice. The modeling data of Figure 8 are from Roland Garwood. The research at California Institute of Technology Jet Propulsion Laboratory was supported by NASA under contract, and the work at the University of Washington was supported by NASA and ONR.

8. REFERENCES

- Brown, R., 1990, Meteorology, in Smith, cd., *Polar Oceanography, Part A, Physical Science*, Academic Press, San Diego, 1-46.
- Carsey, F. and R. Garwood, Identification of modeled ocean plumes in Greenland gyre ERS-1 SAR data, *subm to Geophys. Res. Lett.*, June, 1993).
- Carsey, F., 1992, ed. *Microwave Remote Sensing of Sea Ice*, AGU Monograph 68, 474p.
- Cavalieri, D., J. Crawford, M. Drinkwater, D. Eppler, I. Farmer, R. Jentz, and C. Wackerman, 1991, Aircraft active and passive microwave validation of sea ice concentration from the Defense Meteorological Satellite Program Special Sensor Microwave Imager, *J. Geophys. Res.*, 96, 21,989-22,008.
- Chu, P. and J.-C. Gascard, 1991, eds, *Deep Convection and Deep Water Formation in the Oceans*, Elsevier, 382 p.
- Gascard, J.-C., 1991, Open ocean convection and deep water formation revisited in the Mediterranean, Labrador, Greenland, and Weddell Seas, in Chu, P. and J.-C. Gascard, eds, *Deep Convection and Deep Water Formation in the Oceans*, Elsevier, 382 p.

Grenfell, T., D. Cavalieri, J. Comiso, M. Drinkwater, R. Onstott, I. Rubinstein, K. Steffen, and D. Winebrenner, 1992, Chapter 14. considerations for microwave remote sensing of thin sea ice, in Carsey, F., ed., 1992, *Microwave Remote Sensing of Sea Ice*, AGU Monograph 68, 476 p.

Hollinger, J., J. Pierce and G. Poe, 1990, SSM/I instrument evaluation, *IEEE Trans on Geosci. and Remote Sens.*, 28, 781-790.

Jones, H. and J. Marshall, 1993, Convection with rotation in a neutral ocean: A study of open ocean deep convection, *J. Phys. Oceanogr.*, 23, in press.

Killworth, P., 1979, On chimney formation in the ocean, *J. Phys. Oceanogr.*, 9, 531-554.

Legg, S. and J. Marshall, 1993, A heaton model of the spreading phase of open ocean convection, *J. Phys. Oceanogr.*, 23, in press.

McPhee, M., 1990, Small-scale processes, in Smith, W., ed., *Polar Oceanography, Part A Physical Science*, Academic Press, San Diego, 406P.

Schott, F., M. Visbeck and J. Fischer, 1993, Observations of vertical currents and convection in the central Greenland Sea during the winter of 1988/89, *J. Geophys. Res.*, in press.

Schott, F., M. Visbeck and J. Fischer, 1993, Observations of vertical currents and convection in the central Greenland Sea during the winter of 1988/89, *J. Geophys. Res.*, in press.

Steffen, K., J. Key, D. Cavalieri, J. Comiso, P. Gloersen, K. St. Germain and I. Rubinstein, 1992 in Carsey (ed.) *Microwave remote Sensing of Sea Ice*, AGU Monograph 68, 201-231.

Sutherland, L., R. Shuchman, P. Gloersen, J. Johannessen, and O. Johannessen, 1989, SAR and passive microwave observations of the Odden during MIZEX '87, *IGARSS 1989 Digest*, 1539-1544.

Tucker, W., T. Grenfell, R. Onstott, D. Perovich, A. Gow, R. Shuchman, and L. Sutherland, 1991, Microwave and physical properties of sea ice in the winter marginal ice zone, *J. Geophys. Res.*, 96, 4573-4587.

Wensnehan, M., T. Grenfell, D. Winebrenner, G. Maykut, 1993, Observations and theoretical studies of microwave emission from thin saline ice, *J. Geophys. Res.*, 98, 8531-8546.

Corresponding addresses:

Frank D. Carsey

California Institute of Technology, Jet Propulsion Laboratory, Pasadena CA 911 09;
818-354-8163, F. Carsey/Omnet

and

Andrew T. Roach

Applied Physics laboratory, University of Washington, Seattle WA 98 105; 206-685-7911; A. Roach/Omnet

FIGURE CAPTIONS

Figure 1: Location map for Odden. The numbers at the margin are row and column numbers for a 5 km grid. The numbered circles are Greenland Sea Program Moorings as discussed in Roach et al, 1993. The box encloses the region known as Odden, and the satellite data discussed here is within this box. The western edge of Odden itself is taken to be the dashed line at left. The dashed line that runs nearly up the box is approximately along the section of Bourke et al, 1992, and the solid hooking line outlines their JMC 1.5°C boundary.

Figure 2. SSM/I Data for the centerline of the Odden box on day 17 of 1989. In the upper frame is a plot of T_B vs distance down the box along column 208 of Figure 1. The heavy lines indicate the top and bottom of the Odden box. In the center frame the calculated PR and GR are shown for the profile through the box only. Both of these variables have minimum values in thick consolidated ice. In the bottom frame PR and GR in the box are plotted against each other with different symbols used for different parts of the profile. The presence of old ice would draw GR down; the variation shown is due to either ice concentration or thickness of pancakes.

Figure 3. SSM/I values of 37 GHz PR {Where $PR = (T_{bV} - T_{bH}) / (T_{bV} + T_{bH})$ } for the winter of 1989; day of year numbers are shown above each map. In part A the entire winter is summarized with PR data on 12 day separation. In part B the period of rapid evolution of the Nordbukta (the central ice retreat) is shown with PR data on 2 day separation. In these maps the reds and oranges are open water (with weather), and the blues and greens are ice while yellow is a transition color which can be oceanic if heavy weather is present. The yellow spot to the east of the Nordbukta in days 89034 and following is hypothesized to be a convective sensible-heat polynya.

Figure 4. SSM/I data for 1992 for the Odden region, as in Figures 1 and 3. In part A we show the outline of the region shown in Figure 6 MIS-1 SAR data.

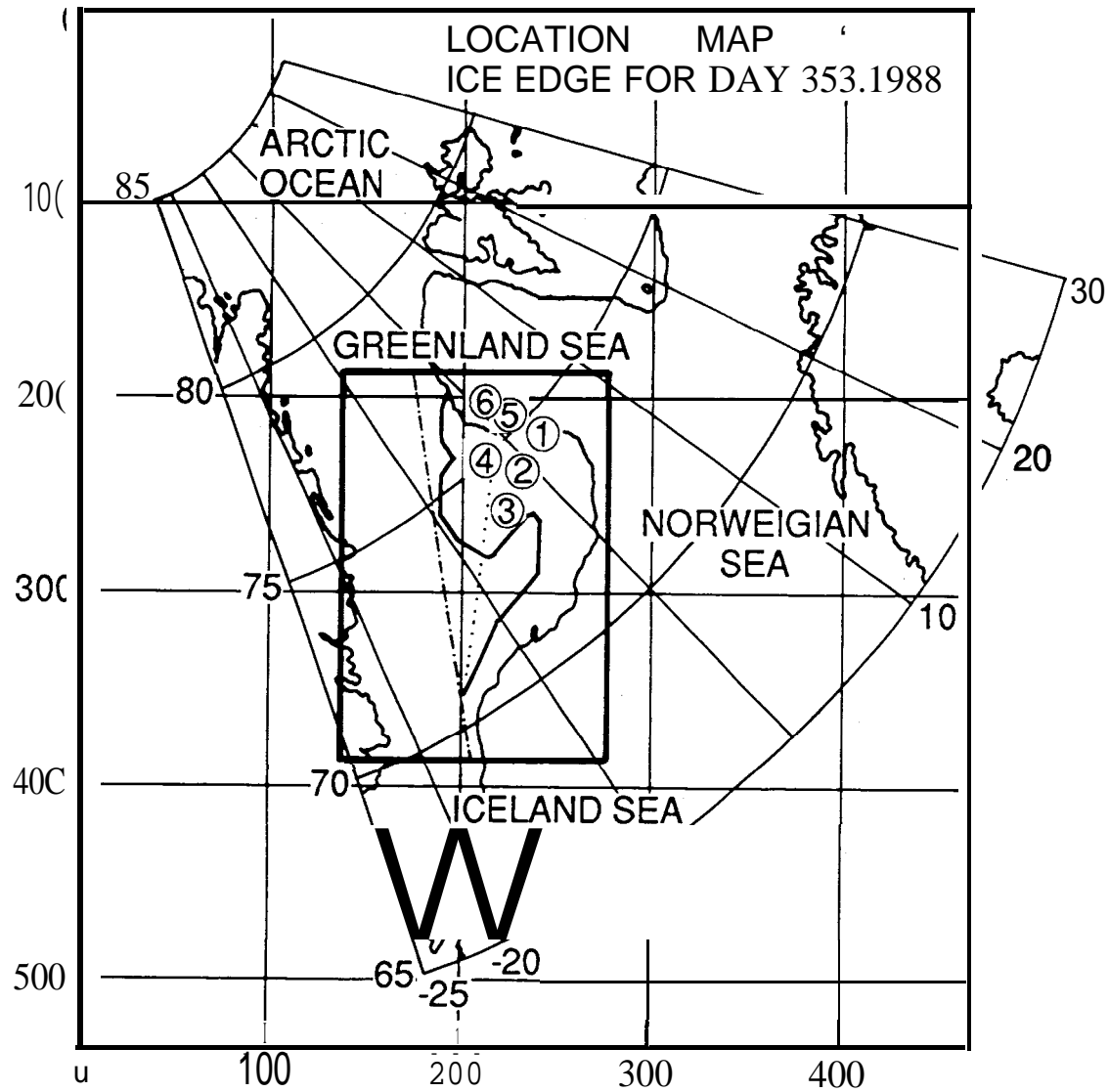
Figure 5. The geometry for the ice edge model. The centerline of the box is seen to have an offset from true north of 44°. G is the geostrophic wind, U is the modeled ice motion and Ux is the component of ice motion down the box centerline.

Figure 6. Ice retreat rates down the box of Fig. 5 in 1988-89 as measured in the SSM/I data and as predicted with a simple wind-driven model. The errors estimated for the model result are about 40% so that a nominal agreement is found.

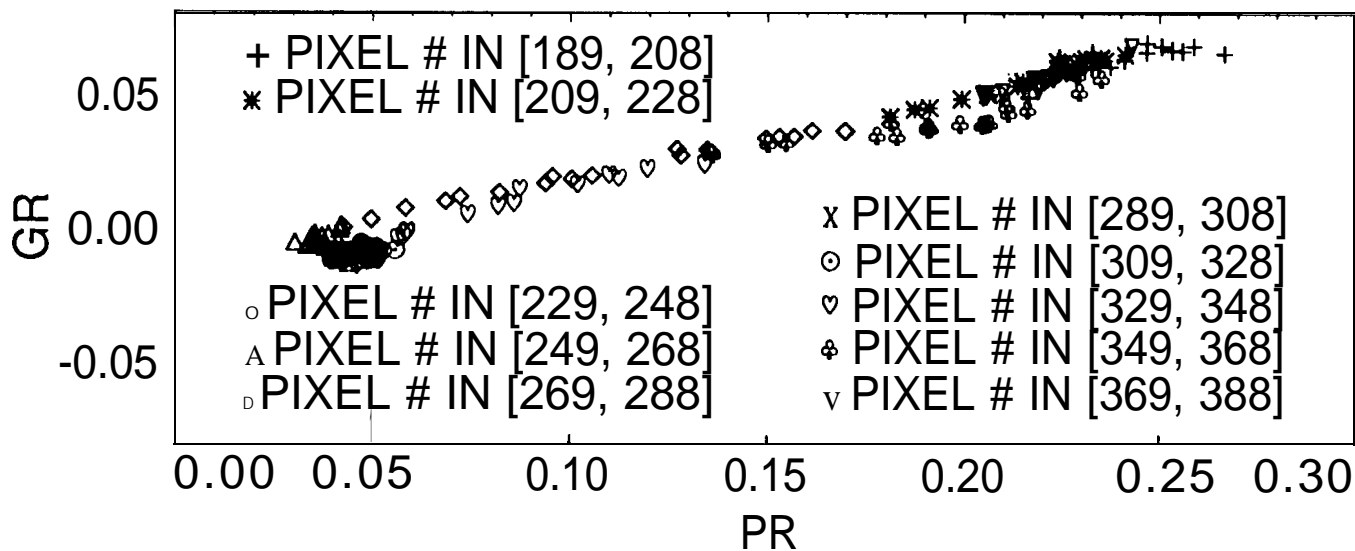
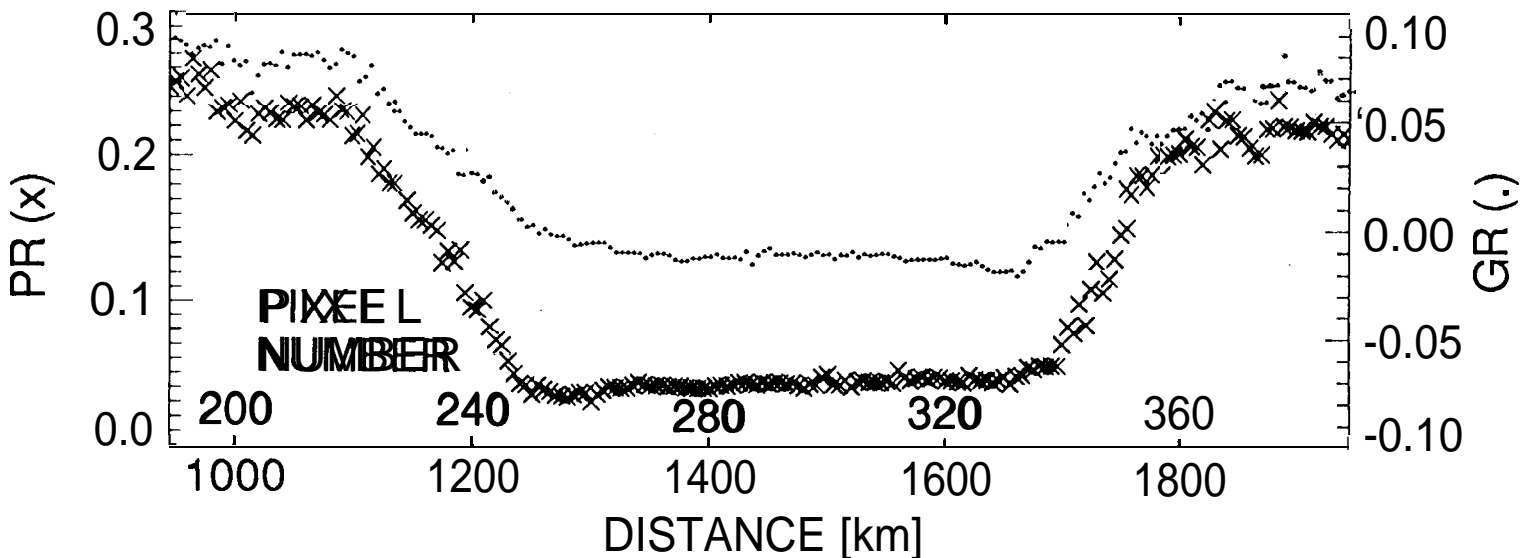
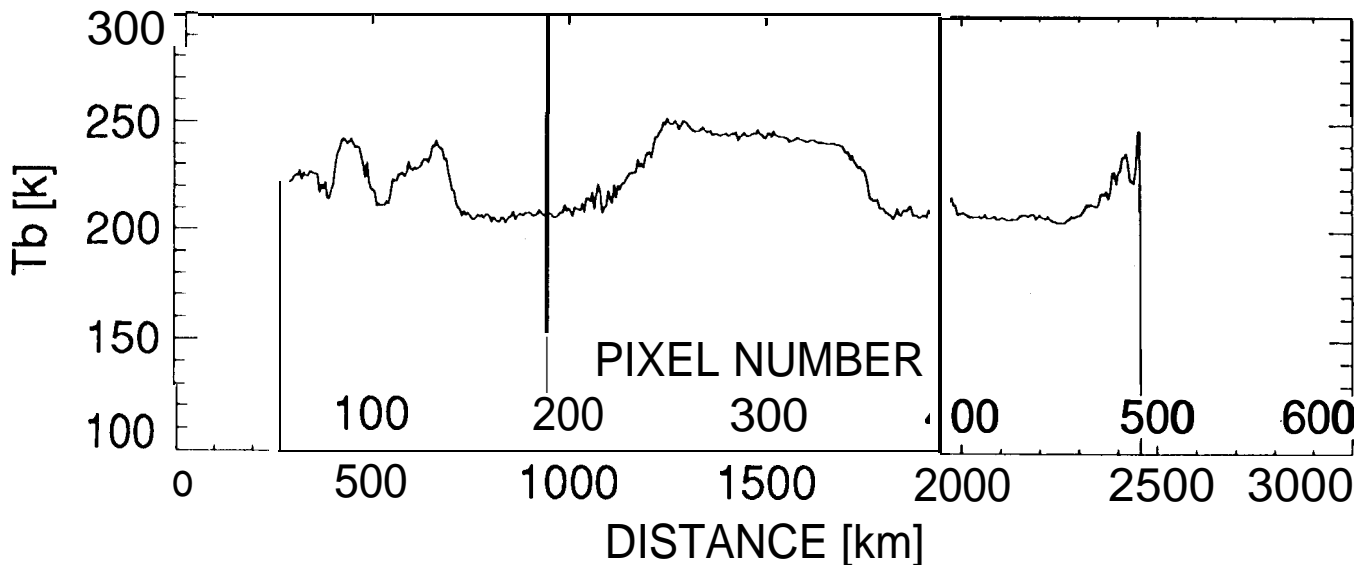
Figure 7. The eastern polynya shown in single-swath 37 GHz SSM/I polarization data over the Odden box for days 35-38 of 1989 with times in GMT. Empty areas were not covered, and empty arcs are bad data. The data are clustered around the times of the ascending and descending passes, near 0200 and 1900 GMT.

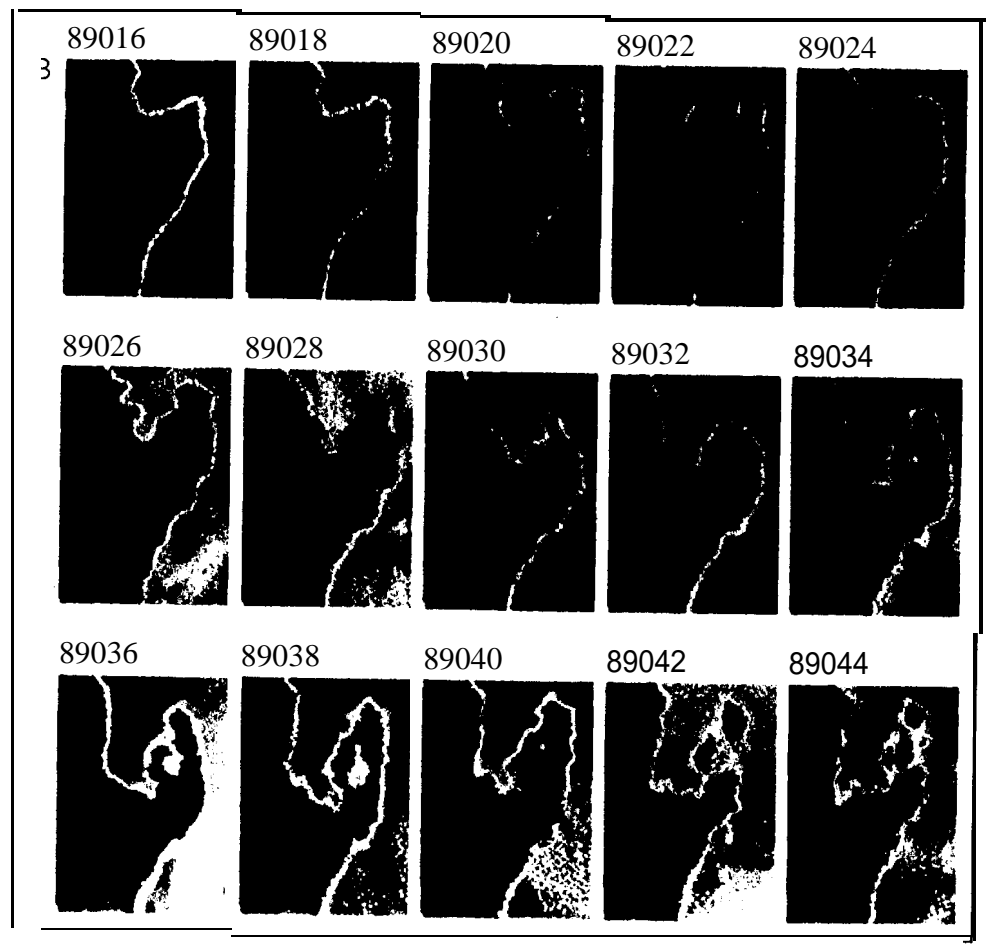
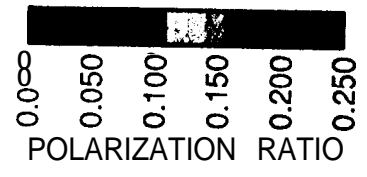
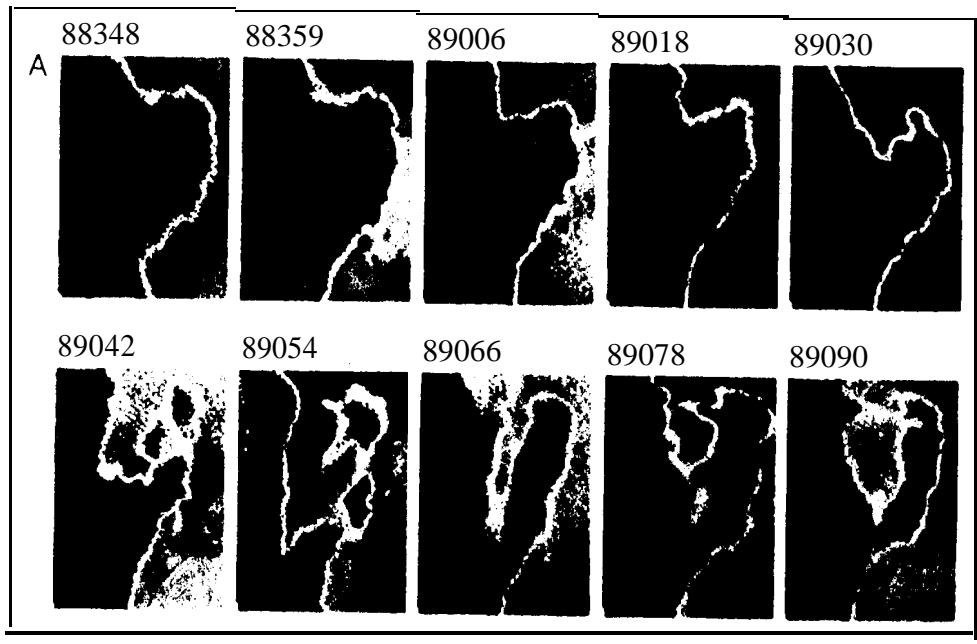
Figure 8. Plumes in the Greenland Sea as modeled (Garwood, 1991) and observed in ERS-1 SAR images (Carsey and Garwood, 1993), 8a is the ERS-1 SAR data at nominal swath of 100 km and reduced resolution, about 100 m; in the blowups of 8b and 8d the resolution is shown at 30 m. The model result only covers an area 3.6 km on a side; four identical such regions are grouped in Figure 8c.

Figure 9. Hypothesized processes in the Nordbukta (A) and in the eastern polynya (B) in cartoon form, not to scale. The role of ice is shown as providing brine for convection; this assumes that the convecting density is approached by adding brine to cold water so that the sinking water will be a bit fresher than the surrounding water.



1989 DAY 17 ALONG CENTER LINE OF ODDEN BOX





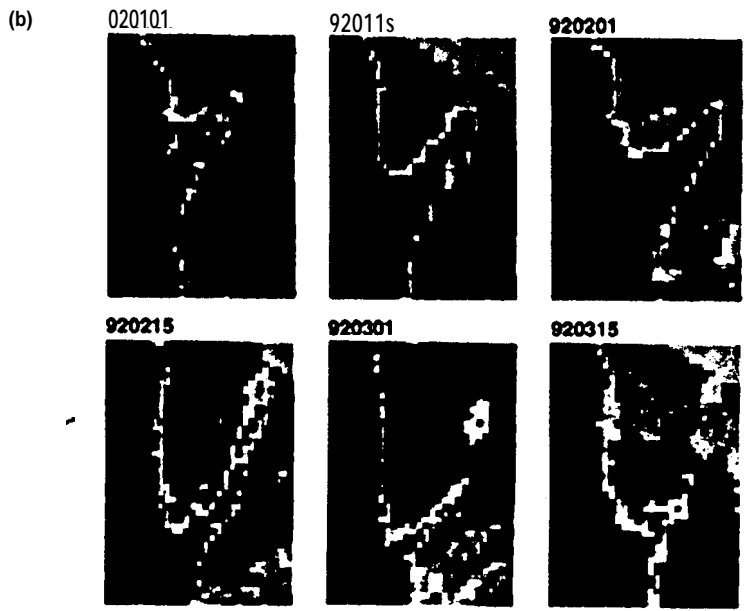
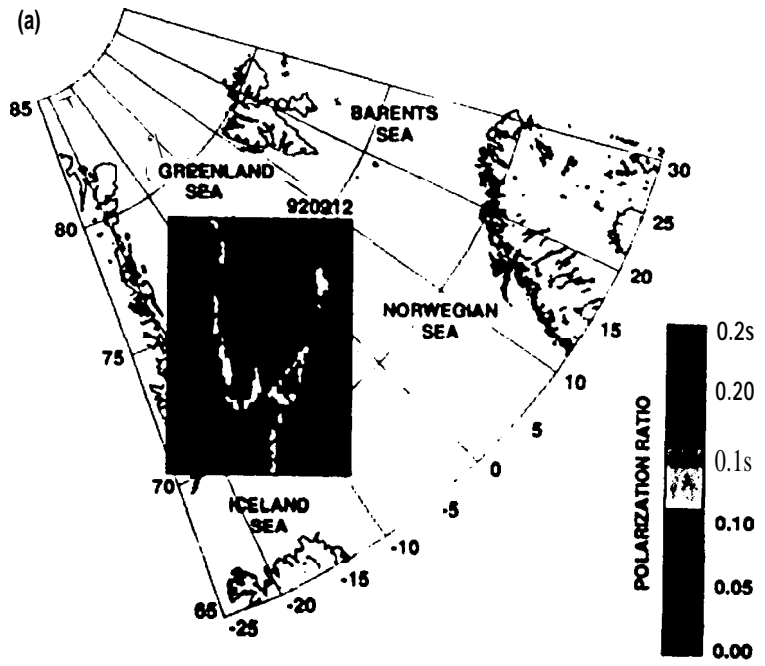
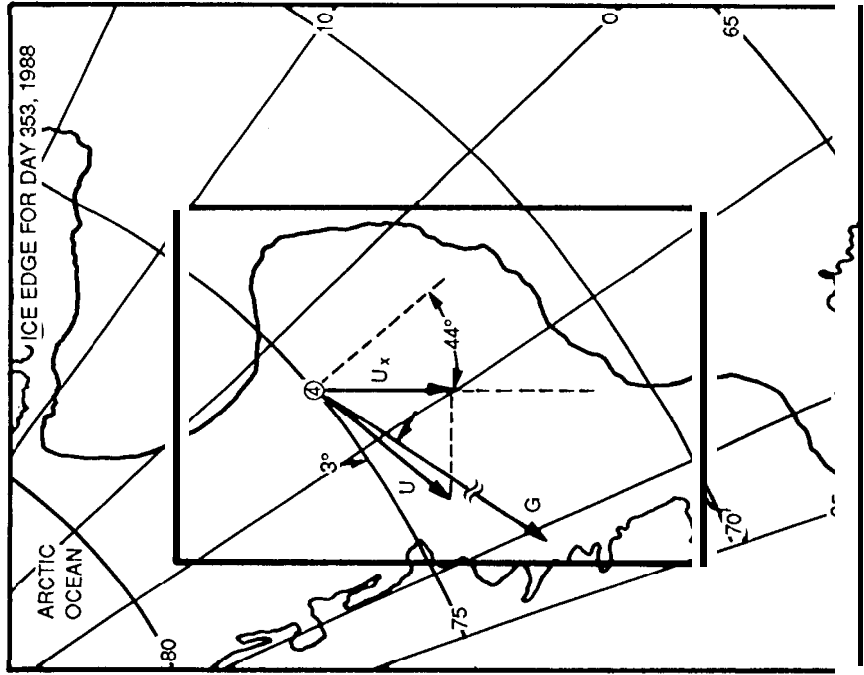
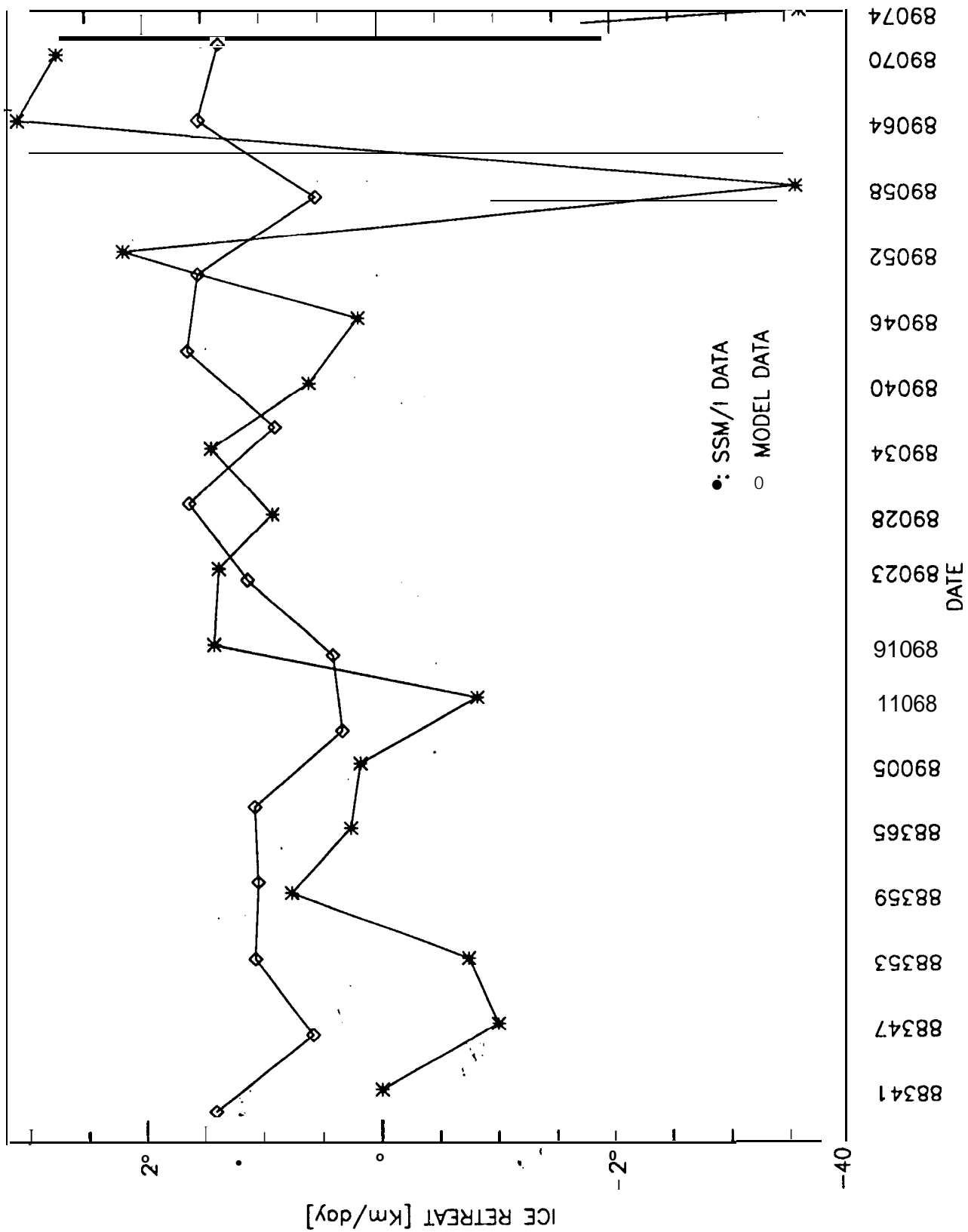


FIG 4



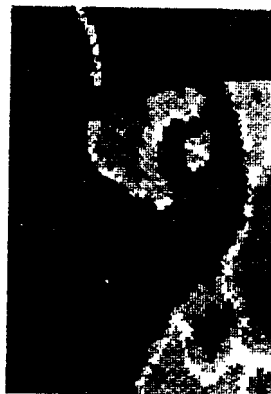
TIME SERIES ON ICE RETREAT COMPARISON



890350321



89(3351847



890352030



890360128



890360308



890370256



890371823



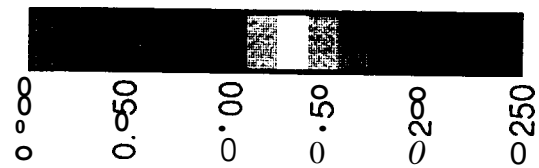
890372004



890380244



890381810



0.00

0.50

0.00

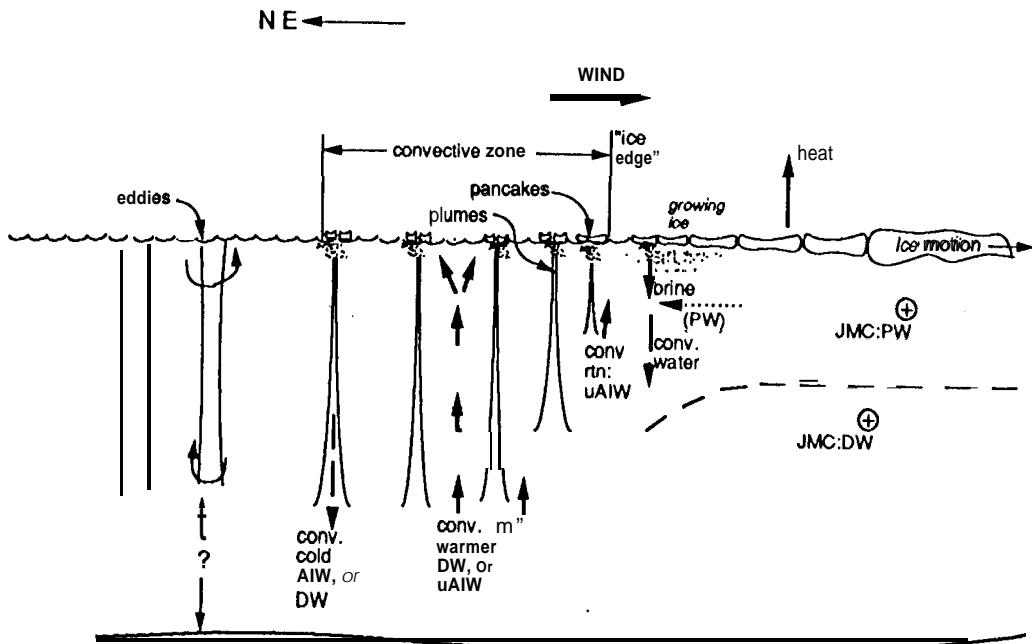
0.50

0.250

0.250

POLARIZATION RATIO

A) CENTRAL RETREAT CONVECTION



B) ODDEN EASTERN-CHIMNEY CONVECTION

